Biophysical Journal, Volume *119*

Supplemental Information

Interplay of Disorder and Sequence Specificity in the Formation of Stable Dynein-Dynactin Complexes

Nikolaus M. Loening, Sanjana Saravanan, Nathan E. Jespersen, Kayla Jara, and Elisar Barbar

Table S1: ITC results for IC interactions with p150^{Glued} CC1B at 25ºC from this and previous papers.

Species	IC Construct	p150^{Glued} CC1B Construct		*n*	K_d (μM)	ΔG^o (kcal/mol)	ΔH^o (kcal/mol)	TΔS^o (kcal/mol)
Rat [Ref. (1)]	IC-2C$_{1–96}$	p150* (contains residues 382–531)		1.1 ± 0.1	13 ± 3	–6.7 ± 0.1	–25 ± 3	–18 ± 3
	IC-2C$_{1–44}$			1.00 ± 0.04	17 ± 2	–6.5 ± 0.1	–16 ± 5	–9 ± 5
Yeast [Ref. (2)]	Pac11$_{1–87}$	Nip100 CC1B		0.97 ± 0.01	5.6 ± 0.1	−7.16 ± 0.01	−8.0 ± 0.5	–0.8 ± 0.5
	Pac11$_{1–87\ Δ66–73}$ (see note a)				> 35 (see note b)			
Drosophila [Ref. (3)]	IC$_{1–87}$	p150$_{221–509}^{Glued}$		0.99 ± 0.02	3.6 ± 0.3	−7.4 ± 0.05	−5.5 ± 0.2	1.9 ± 0.2
	IC$_{1–40}$				> 30 (see note b)			
CT (this study)	IC$_{88}$	p150$_{ABC}$	Step 1	0.49 ± 0.04	0.0020 ± 0.0008	–11.8 ± 0.2	–4.2 ± 0.2	7.6 ± 0.3
			Step 2	0.50 ± 0.04	0.42 ± 0.13	–8.7 ± 0.2	1.9 ± 0.2	10.6 ± 0.2
	IC$_{35}$		Step 1	0.48 ± 0.04	0.009 ± 0.006	–10.9 ± 0.4	–3.9 ± 0.2	7.0 ± 0.4
			Step 2	0.51 ± 0.04	1.3 ± 0.8	–8.0 ± 0.4	0.9 ± 0.2	8.9 ± 0.4
	IC$_{88}$ with rat H2		Step 1	0.47 ± 0.04	0.0045 ± 0.0010	–11.3 ± 0.2	–3.8 ± 0.2	7.5 ± 0.2
			Step 2	0.52 ± 0.05	0.80 ± 0.15	–8.3 ± 0.1	1.8 ± 0.2	10.1 ± 0.2
	IC$_{88}$	p150$_{AB}$			> 30 (see note b)			
		p150$_{BC}$	Step 1		< 0.1 (see note c)			
			Step 2		< 1 (see note c)			
		p150$_{A}$			> 30 (see note b)			
		p150$_{B}$			> 30 (see note b)			
		p150$_{C}$			> 100 (see note d)			

[a]The Pac11$_{1–87\ Δ66–73}$ construct lacks the H2 region (residues 66–73 in yeast IC).
[b]For thermograms in which the binding interaction was too weak to fit reliably, the lower bound for the dissociation constant is provided.
[c]Binding curve only qualitatively fits to a two-site model, so only upper bounds for the dissociation constants are provided.
[d]Binding not observed at the concentrations used for ITC; the lower bound for the dissociation constant is estimated from NMR spectroscopy.

Table S2: Structural statistics for the IC_{88} ensemble

Physical parameters (including nonnative N-terminal residues)	
Number of residues	92
Average molecular weight (unlabeled, Da)	9996.2
Structural restraints	
NOE-derived distance restraints (ARIA cycle 8)	
Intraresidue ($\| i-j \| = 0$)	258
Sequential ($\| i-j \| = 1$)	145
Short ($2 \leq \| i-j \| \leq 3$)	21
Medium ($4 \leq \| i-j \| \leq 5$)	3
Long ($\| i-j \| > 5$)	0
Ambiguous	426
Total	853
Dihedral constraints	
Phi	35
Psi	35
Scalar coupling backbone torsion restraints ($^3J_{HNHA}$)	26
Residual dipolar coupling restraints ($^1D_{HN}$)	17
Statistics for accepted structures	
Accepted structures	20 of 50
Mean CNS energy terms	
E total (kcal mol^{-1})	–2000 (±120)
E van der Waals (kcal mol^{-1})	–130 (±20)
E distance restraints (kcal mol^{-1})	443 (±13)
Restraint violations (average # per structure)	
NOE (> 0.5 Å)	1.7 (±0.8)
Dihedral (> 5º)	0
$^3J_{HNHA}$ (> 1 Hz)	3.1 (±1.1)
$^1D_{HN}$ (> 1 Hz)	2.5 (±0.7)
RMS deviations from the ideal geometry used within CNS	
Bond lengths (Å)	3.26×10^{-3} ($\pm9\times10^{-5}$)
Bond angles (º)	0.476 (±0.015)
Improper angles (º)	1.14 (±0.10)
Dihedral angles (º)	39.9 (±0.3)
Ramachandran statistics [PROCHECK 3.5.4, (4)]	
Most favored (%)	57.2 (±3.6)
Additionally allowed (%)	40.3 (±3.4)
Generously allowed (%)	1.5 (±1.0)
Disallowed (%)	1.0 (±1.2)
MolProbity analyses [v3.19, (5)]	
Clashscore	6.5 (±2.1)
Clashscore percentile (%)	87 (±9)
Clashscore Z-score	1.3 (±0.5)

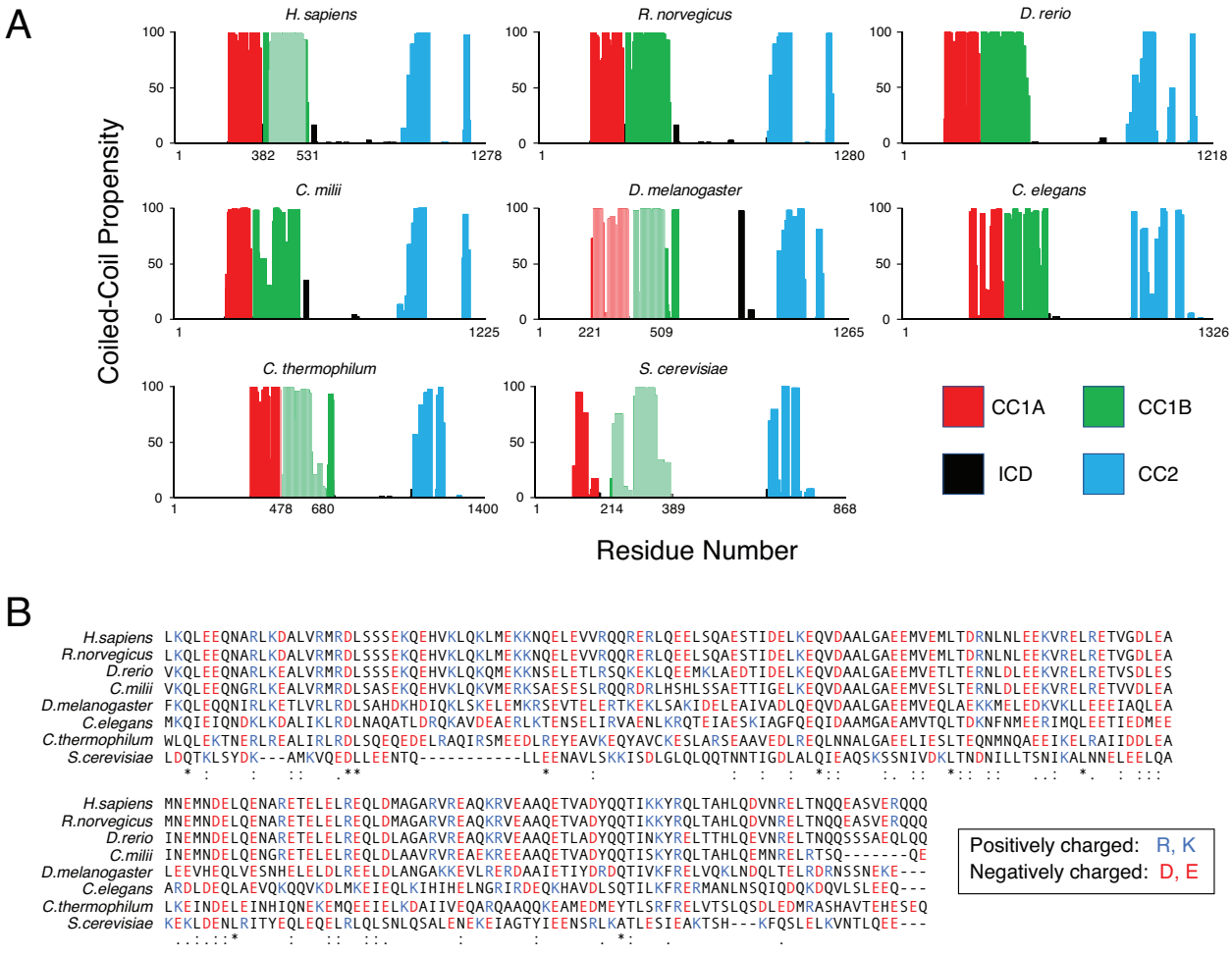

Figure S1: Coiled-coil predictions for dynactin p150^{Glued} and sequence alignment of its CC1B region for eight eukaryotic species.

(A) COILS Server (6) predictions for full length p150^{Glued} from *Homo sapiens* (human), *Rattus norvegicus* (rat), *Danio rerio* (zebrafish), *Callorhinchus milii* (Australian ghostshark), *Drosophila melanogaster* (fruit fly), *Caenorhabditis elegans* (nematode), *Chaetomium thermophilum* (thermophilic fungus) and *Saccharomyces cerevisiae* (yeast). Structural features are highlighted by colors: red (coiled-coil region 1A, CC1A), green (coiled-coil region 1B, CC1B), black (intercoiled domain, ICD), blue (coiled-coil region 2, CC2). The residues used for the *C. thermophilum* p150^{Glued} CC1B construct in this paper and for the *H. sapiens*, *D. melanogaster*, and *S. cerevisiae* p150^{Glued} constructs in other papers (1–3) are shown in light green and light red, and the starting/ending residues of these constructs are indicated on the *x*-axes.

(B) Sequence alignment for the CC1B region of dynactin p150^{Glued} from eight different species made using the MAFFT alignment program (7–9). Identical (asterisk), strongly similar (colon) and weakly similar (period) residues are shown. Residues with positively charged sidechains are indicated in blue and those with negatively charged sidechains are indicated in red.

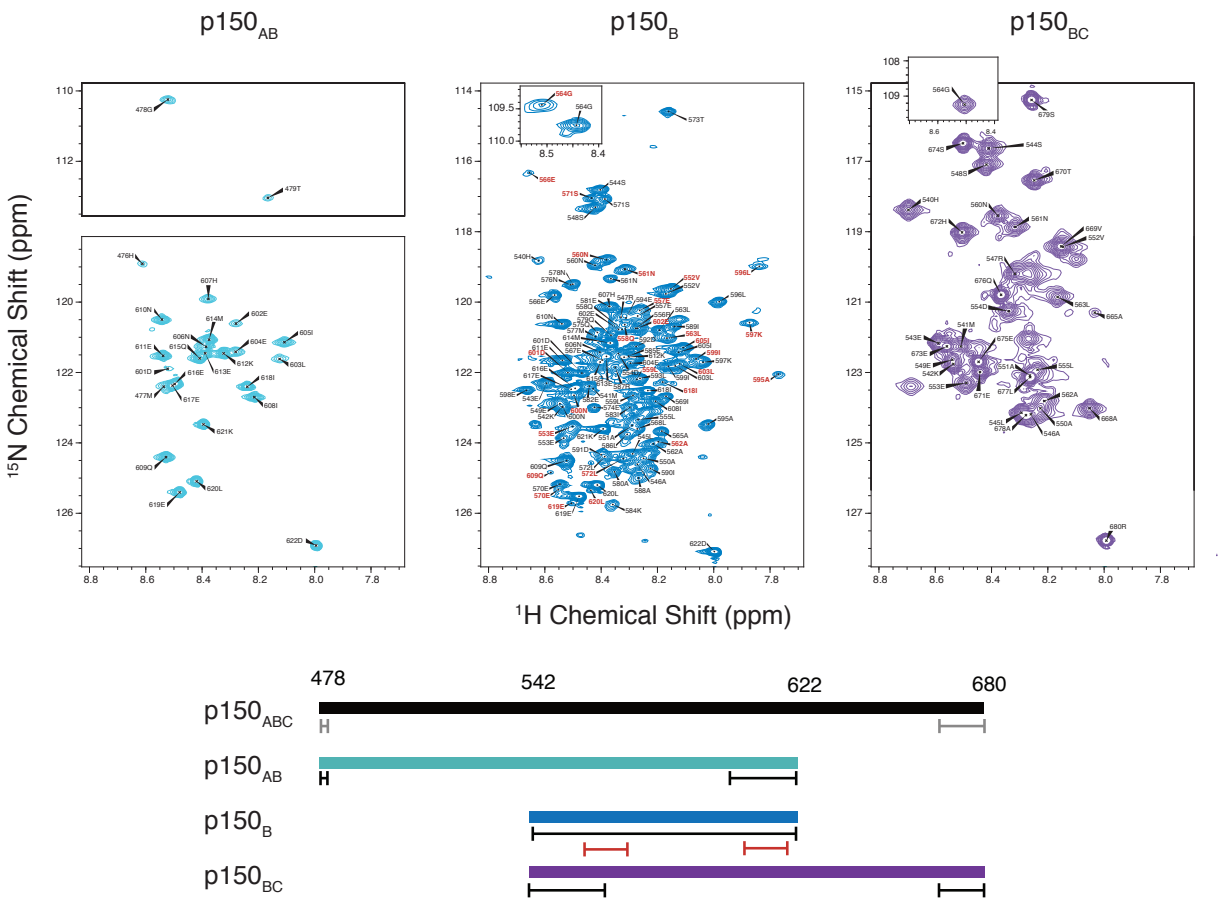

Figure S2: NMR assignments for $p150_{AB}$, $p150_{B}$, and $p150_{BC}$
^{1}H-^{15}N spectra of $p150_{AB}$ (left), $p150_{B}$ (middle), and $p150_{BC}$ (right) were acquired at 800 MHz for ^{1}H. The set of labels for $p150_{B}$ in red indicate peaks from a minor conformation with greater chemical shift dispersion. The diagram at the bottom indicates how the $p150^{Glued}$ constructs studied relate to each other and to the overall ($p150_{ABC}$) sequence. Black brackets indicate regions for which amide residues could be assigned; for all three $p150^{Glued}$ constructs studied by NMR the assignable regions were disordered. Grey brackets indicate which regions are predicted to be disordered for the $p150_{ABC}$ construct, and red brackets indicate regions of $p150_{B}$ for which additional peaks could be observed due to exchange between conformers.

References

1. Jie, J., F. Löhr, and E. Barbar. 2017. Dynein Binding of Competitive Regulators Dynactin and NudE Involves Novel Interplay between Phosphorylation Site and Disordered Spliced Linkers. *Structure*. 25:421–433.

2. Jie, J., F. Löhr, and E. Barbar. 2015. Interactions of Yeast Dynein with Dynein Light Chain and Dynactin: General Implications for Intrinsically Disordered Duplex Scaffolds in Multiprotein Assemblies. *J. Biol. Chem.* 290:23863–23874.

3. Morgan, J.L., Y. Song, and E. Barbar. 2011. Structural dynamics and multiregion interactions in dynein-dynactin recognition. *J. Biol. Chem.* 286:39349–39359.

4. Laskowski, R.A., J.A. Rullmannn, M.W. MacArthur, R. Kaptein, and J.M. Thornton. 1996. AQUA and PROCHECK-NMR: programs for checking the quality of protein structures solved by NMR. *J. Biomol. NMR*. 8:477–486.

5. Chen, V.B., W.B. Arendall, J.J. Headd, D.A. Keedy, R.M. Immormino, G.J. Kapral, L.W. Murray, J.S. Richardson, and D.C. Richardson. 2010. MolProbity: all-atom structure validation for macromolecular crystallography. *Acta Crystallogr D Biol Crystallogr*. 66:12–21.

6. Lupas, A., M. Van Dyke, and J. Stock. 1991. Predicting coiled coils from protein sequences. *Science*. 252:1162–1164.

7. Katoh, K., and D.M. Standley. 2013. MAFFT multiple sequence alignment software version 7: improvements in performance and usability. *Mol. Biol. Evol.* 30:772–780.

8. Li, W., A. Cowley, M. Uludag, T. Gur, H. McWilliam, S. Squizzato, Y.M. Park, N. Buso, and R. Lopez. 2015. The EMBL-EBI bioinformatics web and programmatic tools framework. *Nucleic Acids Res.* 43:W580-584.

9. McWilliam, H., W. Li, M. Uludag, S. Squizzato, Y.M. Park, N. Buso, A.P. Cowley, and R. Lopez. 2013. Analysis Tool Web Services from the EMBL-EBI. *Nucleic Acids Res.* 41:W597-600.